EXPERIMENTAL and MOLECULAR MEDICINE, Vol. 42, No. 9, 614-627, September 2010

TRPC3 cation channel plays an important role in proliferation and differentiation of skeletal muscle myoblasts

Jin Seok Woo[1], Chung-Hyun Cho[2], Do Han Kim[3] and Eun Hui Lee[1,4]

[1]Department of Physiology
College of Medicine
The Catholic University of Korea
Seoul 137-701, Korea
[2]Department of Pharmacology
College of Medicine
Seoul National University
Seoul 110-799, Korea
[3]Department of Life Science
Gwangju Institute of Science and Technology
Gwangju 500-712, Korea
[4]Corresponding author: Tel, 82-2-2258-7279;
Fax, 82-2-532-9575; E-mail, EHUI@catholic.ac.kr
DOI 10.3858/emm.2010.42.9.061

Accepted 19 July 2010
Available Online 19 July 2010

Abbreviations: DHPR, dihydropyridine receptor; EC, excitation-contraction; MDG, muscular dysgenesis; MDG/TRPC3 KD, TRPC3 knock-down in MDG cells; MG29, mitsugumin-29; ROCE, receptor-operated Ca^{2+}-entry; RyR, ryanodine receptor; SOCE, store-operated Ca^{2+}-entry; SR, sarcoplasmic reticulum; STIM, stromal interaction molecule; TRPC, canonical-type transient receptor potential cation channel

Abstract

During membrane depolarization associated with skeletal excitation-contraction (EC) coupling, dihydropyridine receptor [DHPR, a L-type Ca^{2+} channel in the transverse (t)-tubule membrane] undergoes conformational changes that are transmitted to ryanodine receptor 1 [RyR1, an internal Ca^{2+}-release channel in the sarcoplasmic reticulum (SR) membrane] causing Ca^{2+} release from the SR. Canonical-type transient receptor potential cation channel 3 (TRPC3), an extracellular Ca^{2+}-entry channel in the t-tubule and plasma membrane, is required for full-gain of skeletal EC coupling. To examine additional role(s) for TRPC3 in skeletal muscle other than mediation of EC coupling, in the present study, we created a stable myoblast line with reduced TRPC3 expression and without $\alpha1_S$DHPR (MDG/TRPC3 KD myoblast) by knock-down of TRPC3 in $\alpha1_S$DHPR-null muscular dysgenic (MDG) myoblasts using retrovirus-delivered small interference RNAs in order to eliminate any DHPR-associated EC coupling-related events. Unlike wild-type or $\alpha1_S$DHPR-null MDG myoblasts, MDG/TRPC3 KD myoblasts exhibited dramatic changes in cellular morphology (e.g., unusual expansion of both cell volume and the plasma membrane, and multi-nuclei) and failed to differentiate into myotubes possibly due to increased Ca^{2+} content in the SR. These results suggest that TRPC3 plays an important role in the maintenance of skeletal muscle myoblasts and myotubes.

Keywords: calcium channel; dihydropyridine receptor; MG29; Orai1; ryanodine receptor; TRPC3 cation channel; TRPC4 cation channel

Introduction

During membrane depolarization associated with skeletal muscle excitation-contraction (EC) coupling, the L-type Ca^{2+} channel (dihydropyridine receptor (DHPR) in the transverse (t)-tubule membrane) allows entry of extracellular Ca^{2+} and, at the same time, undergoes conformational changes that are transmitted to the internal Ca^{2+}-release channel (ryanodine receptor 1 (RyR1)) in the sarcoplasmic reticulum (SR) membrane causing Ca^{2+} release from the SR to cytoplasm, which finally induces skeletal muscle contraction (Sandow, 1965; Lee *et al*., 2006b; Lee and Allen, 2007). Myotubes derived from $\alpha1_S$DHPR-null muscular dysgenic (MDG) or RyR1-null dyspedic mice show no L-type Ca^{2+} current or no Ca^{2+} transient from the SR, respectively, and subsequently no EC coupling in both cases (Klaus *et al*., 1983; Flucher *et al*., 1993; Nakai *et al*., 1996).

Canonical-type transient receptor potential cation channel 3 (TRPC3) forms homo- and hetero-tetrameric extracellular Ca^{2+}-entry channels of varying current-voltage relationships and activation properties in plasma membrane (Kiselyov and Patterson, 2009). TRPC3 plays important roles in various cells such as immune cells, osteoblastic cells, cardiac myocyte, skeletal muscle cells, smooth muscle cells, neuronal cells, A431 human carcinoma cells, and LNCap prostate cancer cells (Abramowitz and Birnbaumer, 2009; Kiselyov and Patterson, 2009). For example, TRPC3 is a mediator of pathologic cardiac hypertrophy in

mouse myocyte (Wu *et al*., 2010); TRPC3 is required for BDNF (brain-derived neurotrophic factor)-induced elevation of Ca^{2+} at the growth cone and chemo-attractive growth cone-turning (Li *et al*., 2005); TRPC3 mediates uridine triphosphate (UTP)-induced depolarization of smooth muscle cells (Reading *et al*., 2005). In general, TRPC3 can be activated by two different mechanisms: 1) direct modulation by binding of endogenous molecules (for example, activation by diacylglycerol analogues (Hofmann *et al*., 1999; Nilius *et al*., 2008); and, 2) phospholipase C (PLC)-mediated activation through PLC-coupled receptors. The latter mechanism can be sub-divided into two different sub-mechanisms. One is store-operated Ca^{2+}-entry (SOCE) mechanism (for example, when the ER Ca^{2+}-store depletion through inositol 1,4,5-triphosphate (IP_3) receptor by PLC signaling pathway triggers TRPC3 activation) (Li *et al*., 1999; Vazquez *et al*., 2001; Yildirim *et al*., 2005). On the other hand, contradictory studies of TRPC3 mediating SOCE have been reported; TRPC3 acts as a SOCE channel at a relatively lower expression level in DT40 chicken B-lymphocytes (Vazquez *et al*., 2003), but not in HEK293 cells (McKay *et al*., 2000). The other is receptor-operated Ca^{2+}-entry (ROCE) mechanism. For example, in B lymphocytes, when TRPC3 is activated by physical coupling with $PLC\gamma_2$, it is responsible for secondary extracellular Ca^{2+}-entry after B-cell receptor activation (Zhu *et al*., 1998; Nishida *et al*., 2003; Philipp *et al*., 2003). In skeletal muscle, there have been also contradictory studies on TRPC3 as a SOCE channel; TRPC3 is responsible for SOCE in skeletal muscle (Santillan *et al*., 2004), however other groups have suggested that TRPC1 or Orai1 rather than TRPC3 is the SOCE channel (Vandebrouck *et al*., 2002; Sampieri *et al*., 2005; Lee *et al*., 2006a; Lyfenko and Dirksen, 2008). As yet little is known of TRPC3 as a ROCE channel in skeletal muscle.

Skeletal muscle cells (myoblasts and myotubes) express mainly four types of TRPCs: TRPC1, TRPC3, TRPC4, and TRPC6 (TRPC2 with extremely low expression level than others) (Vandebrouck *et al*., 2002; Kiselyov and Patterson, 2009). TRPC1 is involved in maintaining the force during sustained repeated contractions in mouse skeletal muscle (Zanou *et al*., 2010). TRPC1 and TRPC4 form channels anchoring to the dystrophin-associated protein complex and are necessary to maintain the normal regulation of extracellular Ca^{2+}-entry in skeletal muscle (Sabourin *et al*., 2009). Not much is known about TRPC6 function in skeletal muscle. TRPC3 in the t-tubule and plasma membrane of skeletal muscle cells is required for full-gain of skeletal EC coupling (especially for a sustained high Ca^{2+} level at cytoplasm during EC coupling) by allowing extracellular Ca^{2+}-entry (Freichel *et al*., 2005; Pedersen *et al*., 2005; Lee *et al*., 2006a; Ramsey *et al*., 2006; Abramowitz and Birnbaumer, 2009). Expression of TRPC3 in skeletal myoblasts is sharply up-regulated during the early stage of myoblast differentiation into multinucleated myotubes, and it remains elevated in mature myotubes compared with myoblasts (Lee *et al*., 2006a; Abramowitz and Birnbaumer, 2009). TRPC3 physically interacts with several key skeletal muscle proteins such as TRPC1, junctophilin-2, homer1b, mitsugumin-29, calreticulin, and calmodulin as shown by matrix-assisted laser-desorption ionization-time-of-flight mass spectrometry (MALDI-TOF MS) analysis of a chemically cross-linked triadic protein complex from rabbit skeletal triad vesicles and by co-immunoprecipitation assays using primary mouse skeletal myotubes (Woo *et al*., 2008). TRPC3-deficient mice shows impaired walking behavior due to the abnormal skeletal muscle coordination (Hartmann *et al*., 2008). Transgenic mice with TRPC3 over-expression show an increase of extracellular Ca^{2+}-entry resulting in a phenotype of muscular dystrophy causing muscle weakness, wasting, and premature death (Millay *et al*., 2009).

The present study examined possible role(s) of TRPC3 in skeletal muscle other than mediation of EC coupling. We created a stable myoblast line (MDG/TRPC3 KD myoblasts) with reduced TRPC3 expression and without $\alpha 1_S$DHPR expression (by knock-down of TRPC3 in $\alpha 1_S$DHPR-null MDG myoblasts using retrovirus-delivered small interference RNAs) in order to eliminate DHPR-associated EC coupling-related event(s), and examined the characteristics of the MDG/TRPC3 KD myoblasts.

Results

Creation of the MDG/TRPC3 KD myoblast line

To examine possible role(s) of TRPC3 in skeletal muscle other than mediation of EC coupling, we created a stable myoblast line that had reduced expression of TRPC3 and no expression of DHPR by knock-down of TRPC3 in $\alpha 1_S$DHPR-null MDG myoblasts using retrovirus-delivered small interference RNAs. MDG myoblasts that do not express pore-forming $\alpha 1_S$ subunit of DHPR and subsequently have no EC coupling were used to eliminate any DHPR-associated EC coupling-related events. Total mRNA isolated from ten different TRPC3 knock-down and $\alpha 1_S$DHPR-null

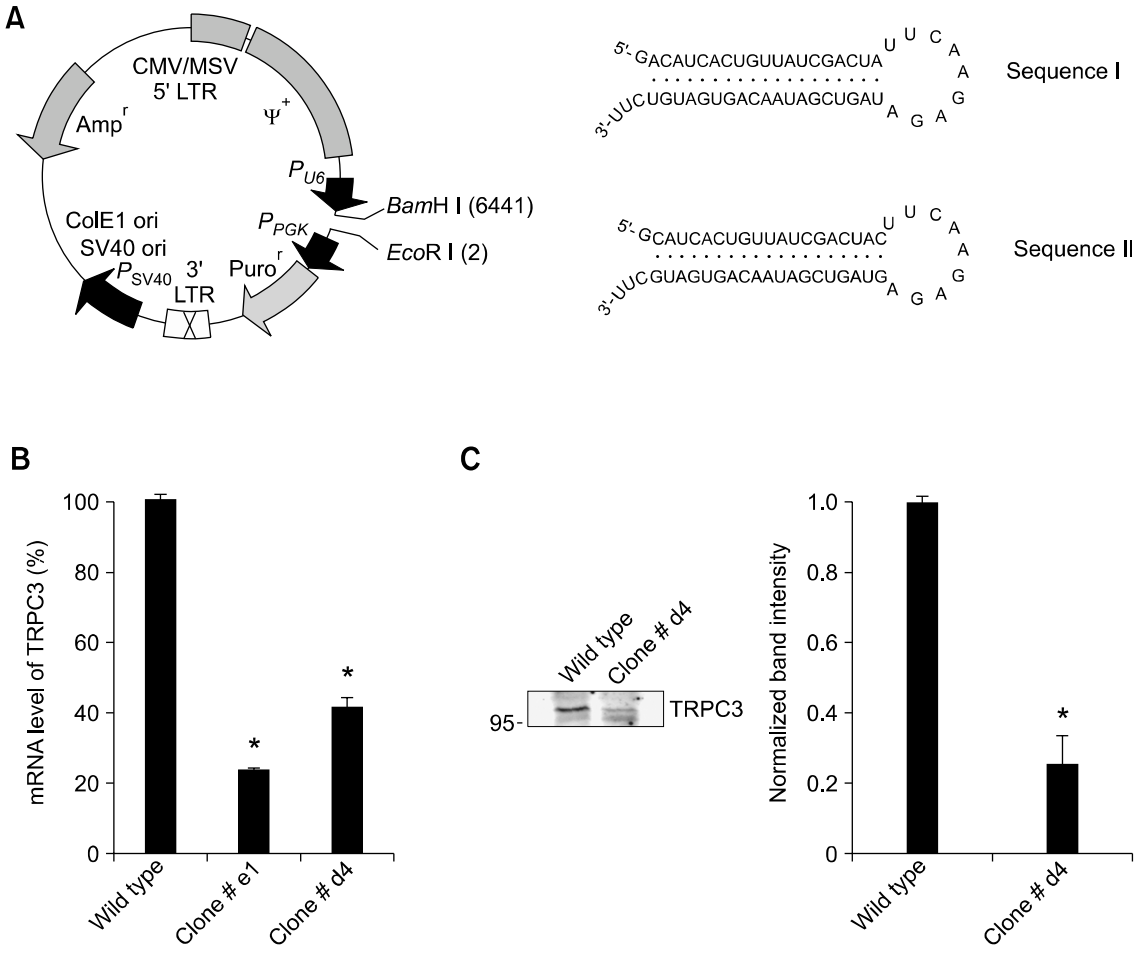

Figure 1. Creation of the MDG/TRPC3 KD myoblast line. (A) To obtain the virus to interfere with TRPC3 mRNA in $\alpha 1_S$DHPR-null MDG myoblasts, a retroviral vector and two different sequences (Sequences I and II) complementary to regions of TRPC3 mRNA were used. The vector map was adapted from the web site of Clontech Laboratories, Inc. P_{PGK}, P_{u6}, and P_{sv40}, PGK, human U6, and SV40 promoters; *Puro*^{r} or *Amp*^{r}, puromycin or ampicillin resistance; 5'-*LTR CMV/MSV*, mouse cytomegalovirus type I and sarcoma virus hybrid promoter; 3'-*LTR*, 3'-MoMuLV LTR with poly(A) region; *SV40* ori and *ColE1 ori*, replication initiation sites; ψ^+, extended packaging signal. (B) Representative real-time PCR results (mRNA levels) for two myoblast clones (clone #e1 and clone #d4) are presented as histograms normalized to TRPC3 mRNA of wild-type controls. Clone #d4 myoblasts exhibited a 58.64 $\pm$ 1.3% reduction in the TRPC3 mRNA level. Results are means $\pm$ SE of triplicate experiments. (C) Solubilized cell lysate from clone # d4 myoblasts (80 μg total proteins) was subjected to SDS-PAGE (10% gel) and immunoblot assay with anti-TRPC3 antibody (left). Histograms are shown for band intensity normalized to that of wild-type controls (right, 75.0 $\pm$ 0.8% reduction in the TRPC3 protein). Results are means $\pm$ SE of three independent experiments. Clone #d4 myoblasts were named MDG/TRPC3 KD myoblasts in all subsequent figures. *Significant difference compared with wild-type ($P < 0.05$).

myoblast clones was subjected to reverse-transcription PCR, and the prepared cDNAs were subjected to real-time PCR to examine TRPC3 mRNA levels. The levels of GAPDH mRNA were used as positive controls. Wild-type myoblasts infected with the empty retroviruses were used as negative controls (data not shown). Real-time PCR results for two different representative clones normalized to that of wild-type myoblasts are presented in Figure 1B (clone #e1 and clone #d4). Clone #e1 was the most effective clone of ten clones (with a 76.4 $\pm$ 1.3% reduction in mRNA level). However, clone #e1 myoblasts were not maintained due to detachment of the myoblasts from the bottom of the culture plates during the third passage. When the reduction in TRPC3 mRNA level was greater than approximately 60%, the results were similar to those observed for clone #e1 myoblasts. Clone #d4 myoblasts showed a 58.64 $\pm$ 1.3% reduction in TRPC3 mRNA level (Figure 1B). Immunoblot assay with anti-TRPC3 antibody of the solubilized cell lysate from clone #d4 myoblasts (80 μg of total protein) showed a 75.0 $\pm$ 0.8% reduction in TRPC3 protein compared with wild-type myoblasts (Figure 1C). Clone #d4 myoblasts showed adequate proliferation. Therefore clone #d4 myoblasts were named MDG/TRPC3 KD myoblasts, and were used in all

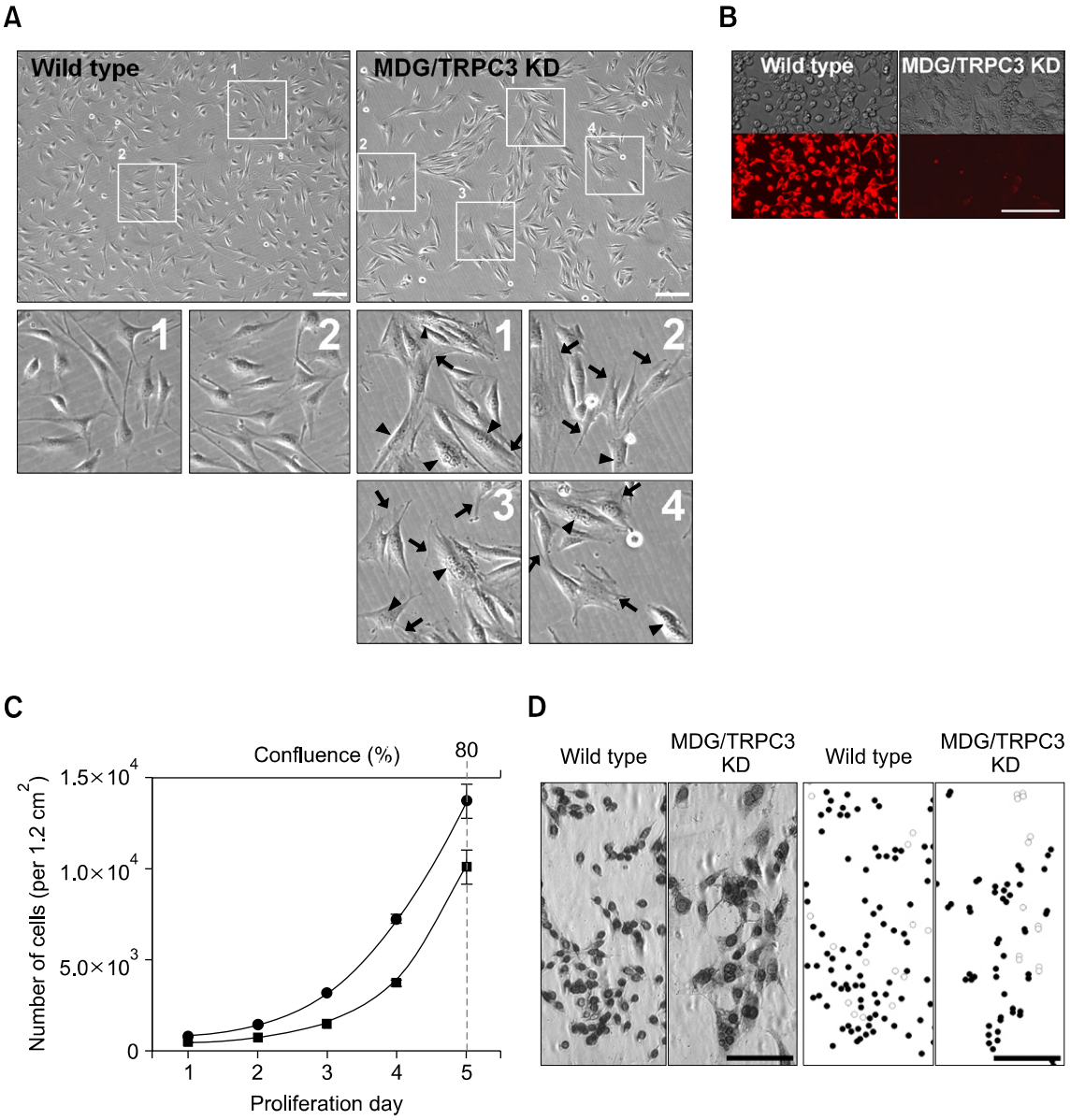

Figure 2. Morphological changes in MDG/TRPC3 KD myoblasts. (A) Images of MDG/TRPC3 KD myoblasts plated on 10-cm dishes coated with collagen were obtained. Myoblasts in numbered boxes were enlarged and are presented in the lower panel (two boxes for wild-type myoblasts and four boxes for MDG/TRPC3 KD myoblasts). MDG/TRPC3 KD myoblasts were much larger than wild-type myoblasts (in both volume and surface areas, as indicated by arrows), and multi-nucleated (indicated by arrow heads). Bar represents 200 μm. (B) Methanol-fixed wild-type or MDG/TRPC3 KD myoblasts grown on optic 96-well plates coated with Matrigel (upper panel) were subjected to immunohistochemistry with anti-desmin antibody and visualized using Cy-3-conjugated anti-mouse IgG antibody (lower panel). Unlike wild-type myoblasts, only indistinct Cy-3 fluorescence was detected in MDG/TRPC3 KD myoblasts. Bar represents 200 μm. (C) The number of wild-type or MDG/TRPC3 KD myoblasts was counted under the microscope. Approximately 80% of confluence was obtained on proliferation day 5 in both wild-type and MDG/TRPC3 KD myoblasts, however the number of MDG/TRPC3 KD myoblasts at approximately 80% confluence was fewer than that of wild-type myoblasts (approximately two thirds of wild-type myoblast population). (D) Proliferation of wild-type and MDG/TRPC3 KD myoblasts was monitored by BrdU assay. Representative BrdU-stained myoblasts were presented on the left panel. The right panel shows schematic figures for BrdU-positive (filled circles) and -negative (open circles) myoblasts on the left panel. Bar represents 100 μm.

subsequent experiments.

Morphological changes in MDG/TRPC3 KD myoblasts

Dramatic changes in cellular morphology were observed in MDG/TRPC3 KD myoblasts grown on 10-cm dishes coated with collagen (Figure 2A). MDG/TRPC3 KD myoblasts were much larger than wild-type myoblasts. The volume was increased at least 1.5-fold, and the surface area was also

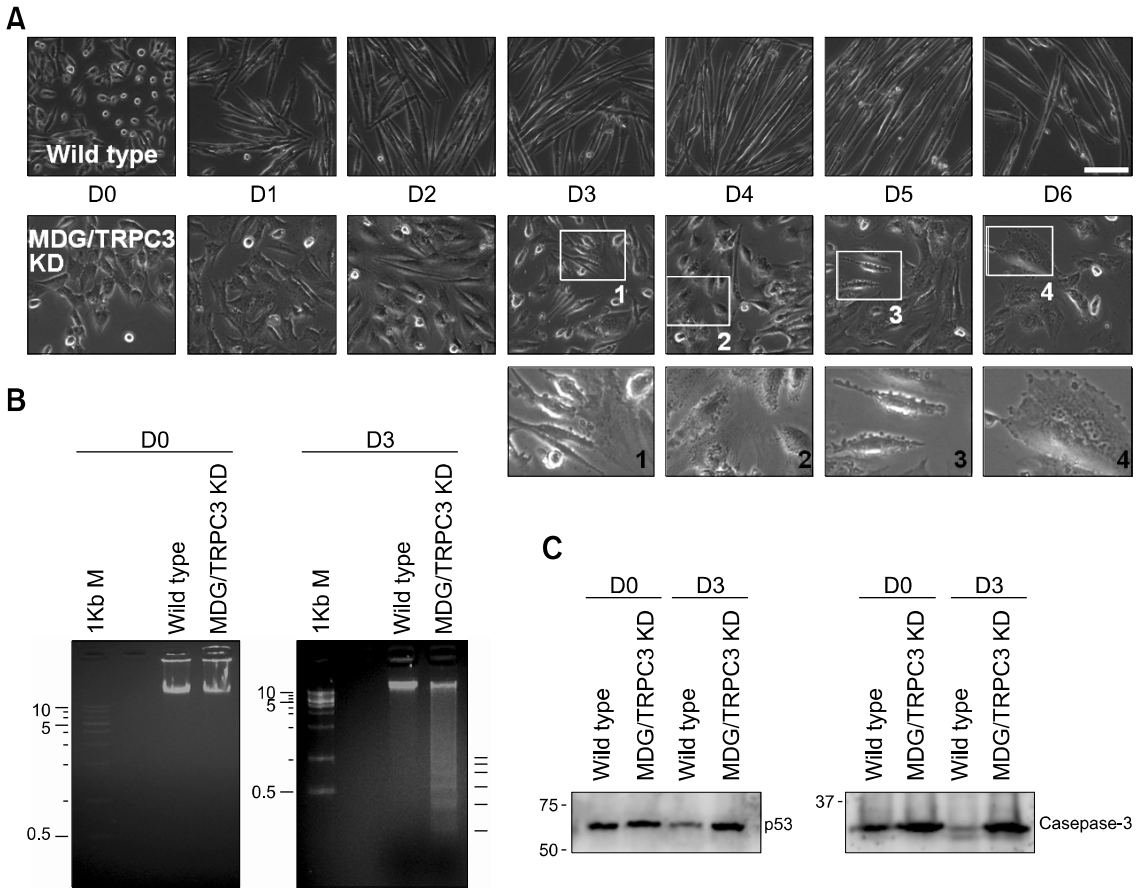

Figure 3. Apoptotic cell death of MDG/TRPC3 KD myoblasts during exposure to differentiation conditions. (A) Fully and successfully differentiated wild-type myoblasts are shown in the upper panel. D0 to D6 means differentiation day zero to six. MDG/TRPC3 KD myoblasts exhibited extensive membrane detachment (brightly circled floating cells) and membrane blebbing (see enlarged images in the third panel) from D3, and finally died during further days. Bar represents 100 μm. (B) Genomic DNA fragmentations, the hallmark of apoptotic cell death, were assessed in wild-type and MDG/TRPC3 KD myoblasts or myotubes on D0 and D3. Intact genomic DNAs of MDG/TRPC3 KD myoblasts on D0 were started to changing to a regularly spaced ladder pattern on D3 by internucleosomal DNA fragmentations (indicated by short bars in the right panel). Wild-type myoblasts or myotubes on the corresponding days were used as positive controls. (C) Solubilized cell lysate from wild-type or MDG/TRPC3 KD cells on D0 or D3 (30 μg of total protein, see Supplemental Data Figure S1) was subjected to SDS-PAGE (10% or 12% gel) followed by immunoblot assay with anti-p53 or anti-caspase-3 antibody. Pro-apoptotic p53 and caspase-3 expressions were highly maintained in MDG/TRPC3 KD cells on D3 compared with those in wild-type cells on D0 or D3.

enhanced due to fine folds in the plasma membrane, as indicated by arrows in Figure 2A. Another outstanding characteristic of the MDG/TRPC3 KD myoblasts was that most, though not all, MDG/TRPC3 KD myoblasts were multi-nucleated (indicated by arrow heads in Figure 2A).

Desmin is a marker protein of contractile cells such as skeletal myoblasts and myotubes (Paulin and Li, 2004). MDG/TRPC3 KD myoblasts grown on optic 96-well plates coated with Matrigel, which were more spherical in shape than those grown in 10-cm dishes coated with collagen, were subjected to immunohistochemistry with anti-desmin antibody and visualized using Cy-3-conjugated anti-mouse IgG antibody (Figure 2B). Cy-3 fluorescence was strongly detected in wild-type myoblasts. However, only indistinct Cy-3 fluorescence was detected in MDG/TRPC3 KD myoblasts, suggesting that MDG/TRPC3 KD myoblasts were significantly different from wild-type skeletal myoblasts, as expected based on the dramatic changes in cellular morphology. In the case of $\alpha 1_S$DHPR-null MDG myoblasts, Cy-3 fluorescence was identical to that of wild-type myoblasts (Tassin *et al*., 1988).

Like wild-type myoblasts, the number of MDG/TRPC3 KD myoblasts in proliferation conditions was gradually increased and reached to approximately 80% of confluence on proliferation day 5 (Figure 2C). However the number of MDG/TRPC3 KD myoblasts at approximately 80% confluence was fewer than that of wild-type myoblasts (approximately two thirds of wild-type myoblast population). In addition, considering that the volume of MDG/TRPC3 KD myoblasts was

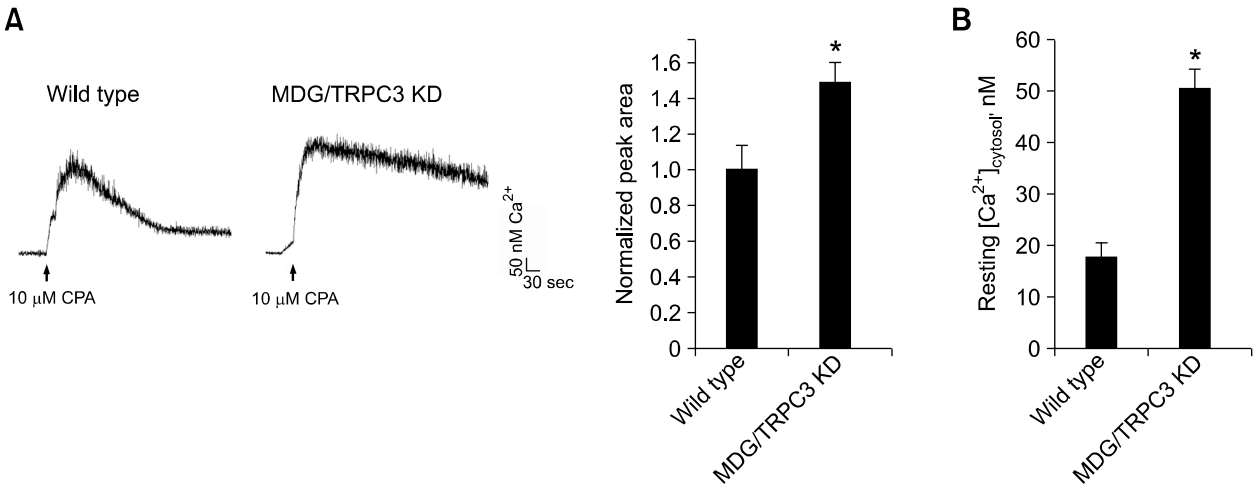

Figure 4. Increases in both the SR Ca^{2+} content and resting cytoplasmic Ca^{2+} level in MDG/TRPC3 KD myoblasts. (A) the SR Ca^{2+} of wild-type or MDG/TRPC3 KD myoblasts loaded with fura-2 was depleted by treatment with 10 μM cyclopiazonic acid (CPA) in the absence of extracellular Ca^{2+}. The peak area for 400 sec normalized to that of wild-type controls is shown in the histograms (right). Results are means ± SE (58 wild-type or 55 MDG/TRPC3 KD myoblasts). Each trace is an average of 4 traces. (B) Resting cytoplasmic Ca^{2+} levels of wild-type or MDG/TRPC3 KD myoblasts are shown as histograms. Results are means ± SE (31 wild-type or 34 MDG/TRPC3 KD myoblasts). Both the SR Ca^{2+} content and resting cytoplasmic Ca^{2+} level were increased in MDG/TRPC3 KD myoblasts. *Significant difference compared with wild-type ($P < 0.05$).

increased at least 1.5-fold (Figure 2A), MDG/TRPC3 KD myoblasts are little reluctant to proliferate compared with wild-type myoblasts. To examine whether MDG/TRPC3 KD myoblasts undergo cell-cycle arrest, bromodeoxyuridine (BrdU, an indicator of cell proliferation) incorporation assay was carried out by adding BrdU to the culture medium. Approximately 85% of myoblasts were positive for BrdU-staining in both wild-type and MDG/TRPC3 KD myoblasts (Figure 2D), suggesting that MDG/TRPC3 KD myoblasts are not permanently arrested in cell cycle in proliferation conditions although it seems that proliferation rate is little slowed down.

Functional changes in MDG/TRPC3 KD myoblasts

MDG/TRPC3 KD myoblasts were subjected to differentiation into myotubes by withdrawal of growth factors (Figure 3A). As expected, wild-type myoblasts differentiated into long, multinucleated myotubes after 5 to 6 days (D5 or D6) in differentiation conditions. MDG/TRPC3 KD myoblasts after exposure to differentiation conditions exhibited severe membrane blebbing (see enlarged images in Figure 3A, third panel), and extensive cell detachment from the bottom of the culture plates (brightly circled floating cells with cellular debris) from D3, and cell death during further days. MDG/TRPC3 KD myoblasts or myotubes on D0 (the same terminology as proliferation day) and on D3 were subjected to the DNA fragmentation assay (Figure 3B). Genomic DNA fragmentations (laddering) in cells are an early stage marker of cell death produced by either apoptosis or by certain stages of necrosis (Alberts, 2008). Wild-type myoblasts or myotubes on the corresponding days were used as positive controls. In case of wild-type myoblasts or myotubes, genomic DNAs on both D0 and D3 were almost intact. However almost intact genomic DNAs of MDG/TRPC3 KD myoblasts on D0 were started changing to a regularly spaced 'ladder pattern' on D3 by internucleosomal DNA fragmentations. Two well-known pro-apototic proteins, p53 and caspase-3 (Soddu *et al*., 1996; Benchimol, 2001; Fernando *et al*., 2002; Siu and Alway, 2005), were examined by immunoblot assay with cell lysate of wild-type or MDG/TRPC3 KD cells on D0 or D3 (Figure 3C): MDG/TRPC3 KD cells on D3 abnormally maintained high expression levels of p53 and caspase-3 compared with wild-type cells on D0 or D3. This is well-accordance with the DNA laddering in Fig. 3B. On the other hand, cell lysate of wild-type or MDG/TRPC3 KD cells on D0 and D3 (30 μg of total protein) was subjected to SDS-PAGE followed by coomassie blue staining in order to check protein expression profiles briefly (Supplemental Data Figure S1). There was no big difference in protein expression profiles between wild-type and MDG/TRPC3 KD cells on D0. Unlike cell lysate on D0, there were significant changes in the protein expression profiles between wild-type and MDG/TRPC3 KD cells on D3: significantly reduced or increased protein bands, suggesting that MDG/TRPC3 KD myoblasts already started to

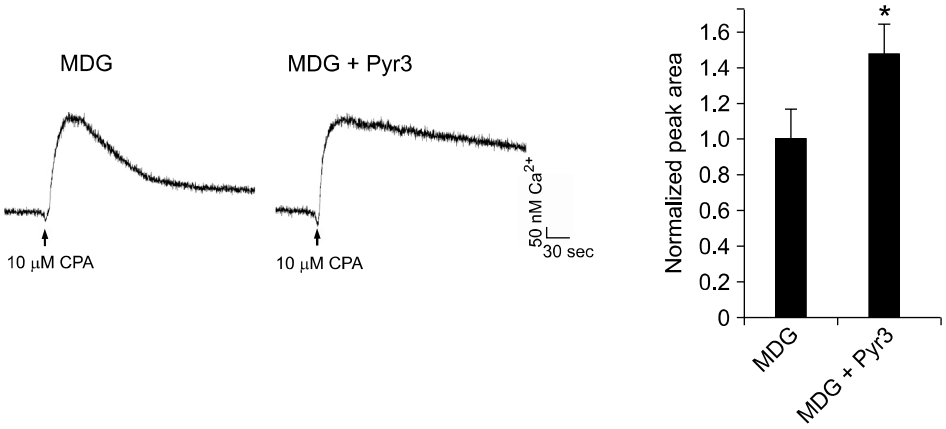

Figure 5. An increase in the SR Ca^{2+} content in MDG myoblasts in the presence of Pyr3, a specific blocker of TRPC3. The SR Ca^{2+} of MDG myoblasts loaded with fura-2 was depleted by treatment with 10 μM CPA in the absence of extracellular Ca^{2+} and presence of 1 μM Pyr3. The peak area for 400 sec normalized to that of wild-type controls is shown in the histograms (right). Results are means ± SE (72 or 78 MDG myoblast for the absence or presence of Pyr3, respectively). Each trace is an average of 4 traces. *Significant difference compared with wild-type ($P < 0.05$).

undergo different processes from those in wild-type myoblasts in differentiation conditions. All these results support that MDG/TRPC3 KD myoblasts in differentiation conditions undergo apoptosis and a subsequent failure in differentiation to myotubes.

Next, to address possible reasons for the defects of MDG/TRPC3 KD myoblasts in differentiation, we firstly estimated the SR Ca^{2+} content (per unit area) in MDG/TRPC3 KD myoblasts by direct treatment with 10 μM cyclopiazonic acid (CPA), which is an inhibitor of the SR Ca^{2+} pump (SERCA1) and, thus, allows for measurement of the SR Ca^{2+} content (Sandow, 1965; Van Assche *et al*., 2007) (Figure 4A). To avoid any possible involvement of extracellular Ca^{2+}-entry by the depletion of the SR Ca^{2+} during CPA treatment (SOCE), the experiment was conducted in the absence of extracellular Ca^{2+}. To analyze intracellular Ca^{2+} transients resulted from CPA treatment, the peak area for 400 sec was considered. There was a significant increase in the SR Ca^{2+} content of MDG/TRPC3 KD myoblasts compared with wild-type myoblasts (a 1.49 ± 1.11-fold increase relative to wild-type myoblasts). To confirm this result, a specific TRPC3 blocker, ethyl-1-(4-(2,3,3-trichloroacrylamide)phenyl)-5-(trifluoromethyl)-1H-pyrazole-4-carboxylate (Pyr3) (Kiyonaka *et al*., 2009), was pre-treated to MDG myoblasts before CPA treatment (Figure 5). MDG myoblasts in the presence of Pyr3 theoretically mimic the genetic ablation of TRPC3 in MDG myoblasts (MDG/TRPC3 KD myoblasts). Indeed, Pyr3 treatment to MDG myoblasts showed an increased SR Ca^{2+} content under the CPA treatment (a 1.47 ± 1.17-fold increase relative to Pyr3-untreated MDG myoblasts). Resting cytoplasmic Ca^{2+} levels in MDG/TRPC3 KD myoblasts were measured (Figure 4B). A significant increase in resting cytoplasmic Ca^{2+} level was also observed in MDG/TRPC3 KD myoblasts compared with wild-type myoblasts (50.5 ± 3.7 nM Ca^{2+} vs. 18.3 ± 2.4 nM Ca^{2+}, respectively). Therefore MDG/TRPC3 KD myoblasts have a much larger

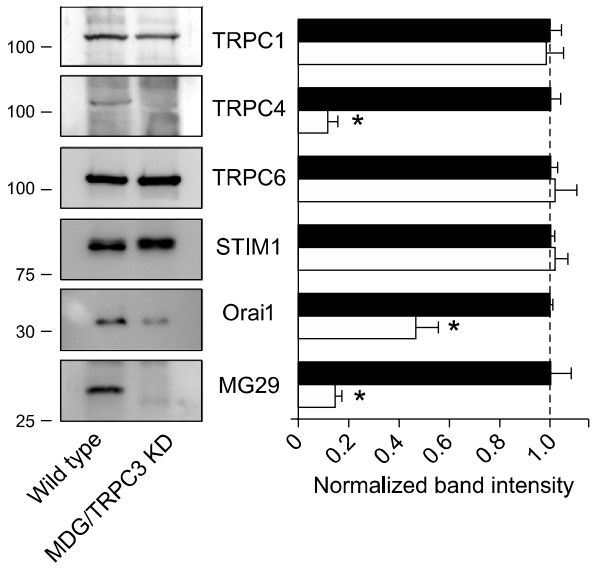

Figure 6. Decreases in the expression level of TRPC4, Orai1, and MG29 in MDG/TRPC3 KD myoblasts. Solubilized cell lysate from wild-type or MDG/TRPC3 KD myoblasts (30 μg of total protein) was subjected to SDS-PAGE (10% or 12% gel) and immunoblot assay with anti-TRPC1, anti-TRPC4, anti-TRPC6, anti-STIM1, anti-Orai1, or anti-MG29 antibody. In MDG/TRPC3 KD myoblasts, the expression of TRPC4, Orai1, and MG29 were dramatically reduced. Results are means ± SE of three independent experiments. *Significant difference compared with wild-type ($P < 0.05$).

Table 1. Characteristics of wild-type, MDG, and MDG/TRPC3 KD myoblasts.

	Wild type myoblast	MDG myoblast	MDG/TRPC3 KD myoblast
Proliferation	Normal	Normal (Flucher *et al*., 1993)	Normal (little reluctant)
Cell size	Normal	Normal (Flucher *et al*., 1993)	Increase
Nucleus	Single	Single (Flucher *et al*., 1993)	Single or multiple
Desmin staining	Positive	Positive (Flucher *et al*., 1993)	Nearly negative
Resting cytosolic Ca^{2+} level	Normal	Increase (Supplemental Data Figure S3B)	Increase
SR Ca^{2+} content	Normal	Normal (Supplemental Data Figure S3A)	Increase
Differentiation	Normal	Normal (Flucher *et al*., 1993)	Failure (apoptosis)

amount of Ca^{2+} in both the SR and resting cytoplasm.

To test whether the increased Ca^{2+} level in the SR and resting cytoplasm in MDG/TRPC3 KD myoblasts affect the expression profile of other proteins, especially RyR1 and DHPR, or vice versa, Ca^{2+} transients were examined in single MDG/TRPC3 KD myoblasts. Caffeine (a direct RyR1 agonist) or KCl (a DHPR activator by inducing membrane depolarization) was applied to wild-type or MDG/TRPC3 KD myoblasts loaded with fura-2 (Supplemental Data Figure S2). In accordance with the fact that skeletal muscle cells in myoblast stage do not express RyR1 and DHPR (Tanaka *et al*., 2000), there was no Ca^{2+} transient in both wild-type and MDG/TRPC3 KD myoblasts in response to caffeine or KCl. Secondly, expression of several proteins known to be expressed in skeletal myoblasts was examined by immunoblot assay (Figure 6). TRPC4, Orai1 (a SOCE-mediating extracellular Ca^{2+}-entry channel (Stiber *et al*., 2008; Vig *et al*., 2008)), and mitsugumin-29 (MG29 (Weisleder *et al*., 2006; Zhao *et al*., 2008)) were significantly down-regulated in MDG/TRPC3 KD myoblasts compared with wild-type myoblasts, however, expression level of TRPC1, TRPC6, and stromal interaction molecule 1 (STIM1, an Orai1-interacting and SOCE-mediating protein (Stiber *et al*., 2008; Vig *et al*., 2008)) were not significantly changed.

Discussion

TRPC3 and DHPR could be a system of checks and double-checks for skeletal myoblast differentiation by playing a redundant role

Previously, we knocked down TRPC3 in primary skeletal myoblasts and myotubes, and found that TRPC3 was required for full gain of skeletal EC coupling, especially for a sustained high Ca^{2+} level at cytoplasm during EC coupling (Lee *et al*., 2006a). In the present study that is part of our continuing series focusing on the role(s) of TRPC3 in skeletal muscle, we examined the possible role(s) of TRPC3 in skeletal muscle other than mediation of EC coupling. Thus, we knocked down TRPC3 in EC coupling-free myoblasts ($\alpha 1_S$DHPR-null MDG myoblasts), clonally selected knock-down myoblasts (MDG/TRPC3 KD myoblasts), and examined the characteristics of MDG/TRPC3 KD myoblasts. MDG/TRPC3 KD myoblasts under double-ablation of extracellular Ca^{2+}-entry channels exhibited dramatic changes in cellular morphology and increases in the SR Ca^{2+} content and the resting cytoplasmic Ca^{2+} level. Moreover, MDG/TRPC3 KD myoblasts lost general characteristics of skeletal myoblasts considering the extremely down-regulated expression of desmin and the failure to differentiate into myotubes (Table 1). In skeletal muscle, TRPC3 and DHPR, two different extracellular Ca^{2+}-entry channels, exhibit different timetable for expression during differentiation: TRPC3 expression is sharply up-regulated from a certain level during the early stage of myoblast differentiation (Lee *et al*., 2006a; Woo *et al*., 2008), and DHPR expression gradually appears and increases during differentiation (Tanaka *et al*., 2000). It seems that TRPC3 and DHPR (and/or Ca^{2+}-entry through the two channels) play a redundant role in myoblasts differentiation such as a system of checks and double-checks. This possibility could explain how myoblasts under single ablation of either TRPC3 or DHPR differentiate well to myotubes (Flucher *et al*., 1993; Lee *et al*., 2006a; Woo *et al*., 2008) - TRPC3 knock-down myoblasts could differentiate well to myotubes possibly due to compensations by the gradual increase of DHPR expression during differentiation; $\alpha 1_S$DHPR-null MDG myoblasts could also differentiate well to myotubes possibly due to compensations by the sharply up-regulated TRPC3 expression during the early stage of myoblast differentiation; double-ablation of TRPC3 and DHPR in MDG/TRPC3 KD myoblasts could induce a failure in differentiation to myotubes.

TRPC3 could be involved in aging processes of skeletal muscle

According to the fact that muscle cells in myoblast stage do not express major proteins for EC coupling such as Ca^{2+} channels (DHPR and RyR1) in sufficient amounts to measure ionic movement (Tanaka *et al*., 2000) (Supplemental Data Figure S2), which does not allow us to examine electrophysiological characteristics of MDG/TRPC3 KD myoblasts such as patch-clamp or single channel current measurement, we compared the cellular morphology and Ca^{2+} levels in the SR and in resting cytoplasm between wild-type and MGD/TRPC3 KD myoblasts. Morphology in MDG/TRPC3 KD myoblasts, such as expansion in both cell volume and plasma membrane and multi-nuclear arrangement, differed significantly from those in wild-type myoblasts. MDG/TRPC3 KD myoblasts looked rather like fused and multinucleated myo'*tubes*'. However MDG/TRPC3 KD myoblasts also differed from wild-type myo'*tubes*'. The MDG/TRPC3 KD myoblasts expanded in all directions, rather than the typical longitudinal and tubular expansion of wild-type myotubes. Unlike the multinuclear arrangement of differentiated wild-type myotubes somewhat like peas in a pod, the multiple nuclei of MDG/TRPC3 KD myoblasts were clustered at the myoblast centers. There are three possible explanations for these unusual characteristics of MDG/TRPC3 KD myoblasts. Firstly, it is possible that the multinucleation in MDG/TRPC3 KD myoblasts may be induced by a defect in cytoplasmic division (no correlation between mitosis and cytokinesis during mitotic phase of the cell cycle) due to the ablation of extracellular Ca^{2+}-entry channel, TRPC3. DHPR is of no relevance to the unusual characteristics of MDG/TRPC3 KD because muscle cells in the myoblast state do not express DHPR (Tanaka *et al*., 2000). If this is the case, MDG/TRPC3 KD myoblast clones should become extinct after several passages. However, MDG/TRPC3 KD myoblasts were well-maintained under proliferation conditions except for certain reluctance. In addition, in case of HeLa cells, extracellular Ca^{2+}-entry by SOCE mechanism is rather suppressed during mitotic phase of the cell cycle (Preston *et al*., 1991). The second possibility is that the relatively long-term culture for single myoblast cloning process of MDG/TRPC3 KD myoblasts could induce myoblasts that are entirely different from wild-type myoblasts. However, this possibility is unlikely because coomassie blue staining of the myoblast lysate showed that the overall profile of protein expression in MDG/TRPC3 KD myoblasts was not dramatically altered compared with that of wild-type or MDG myoblasts. The third possibility is that MDG/TRPC3 KD myoblasts become senescent. This possibility is supported by symptoms of senescence in MDG/TRPC3 KD myoblasts when they were exposed to differentiation conditions: characteristics of apoptotic cell death such as increases in the cytoplasmic Ca^{2+} level, membrane blebbings, cell detachments, cell fragmentations resulting in cellular debris, genomic DNA fragmentations, and finally cell death (Alberts, 2008). In case of neuronal cells, it has been reported that down-regulation of TRPC3 with TRPC6 in neonatal rat cerebellum induces the apoptosis of cerebellar granule neurons (Jia *et al*., 2007).

Considering that MDG/TRPC3 KD myoblasts become senescent when exposed to differentiation conditions, until now mitsugumin-29 (MG29), might be the best clue to access how TRPC3 is involved in the senescence of skeletal muscle. Aged skeletal muscle displays decreased MG29 expression and reduced SOCE (Weisleder *et al*., 2006; Zhao *et al*., 2008), and fibers isolated from MG29 knock-out young mice also show reduced SCOE (Brotto *et al*., 2004). MG29 is one of TRPC3-interacting proteins (Woo *et al*., 2008). Of interest, MG29 expression was extremely decreased in MDG/TRPC3 KD myoblasts compared with wild-type myoblasts. Therefore TRPC3 accompanied by MG29 could be involved in aging processes of skeletal muscle.

TRPC4 and Orai1 could be functional partners of TRPC3 in maintaining the SR Ca^{2+} content of skeletal myoblasts

Like MDG/TRPC3 KD myoblasts (missing of DHPR 'and' reduced expression of TRPC3), $\alpha 1_S$DHPR-null MDG myoblasts (only missing DHPR) also had increased resting cytoplasmic Ca^{2+} levels (Supplemental Data Figure S3). However $\alpha 1_S$DHPR-null MDG myoblasts have normal SR Ca^{2+} content and morphology compared with wild-type myoblasts (Supplemental Data Figure S3), and differentiate well into myotubes (Flucher *et al*., 1993), suggesting that normal SR Ca^{2+} content is one of key factor for the maintenance of skeletal muscle cells (i.e. normal proliferation and differentiation) and that TRPC3 could contribute to maintaining the normal SR Ca^{2+} content in skeletal myoblasts. Heterologously expressed TRPC3s in HEK293 cells form internal Ca^{2+}-release channels in the ER membrane like IP3 receptors and lower the ER Ca^{2+} content (Lof *et al*., 2008). Similarly, a low Ca^{2+} content in the ER accompanies up-regulation of TRPC3 expression in LNCap prostate cancer cell (Pigozzi *et al*., 2006). Therefore it is

very possible that, reversely, down-regulation of TRPC3 by knock-down of TRPC3 in MDG myoblasts could induce a high SR Ca^{2+} content in MDG/TRPC3 KD myoblasts. These phenomenological similarities suggest that increases or decreases in SR/ER Ca^{2+} content are not directly nor positively related to the expression level of extracellular Ca^{2+}-entry channels. In case of TRPC3 knock-down myo'tubes' (Lee *et al*., 2006a), DHPR could possibly compensate for the TRPC3 knock-down effect on the SR Ca^{2+} content and subsequently allow normal SR Ca^{2+} content and normal morphology of myotubes during differentiation.

MDG/TRPC3 KD myoblasts showed no change in the expression of two TRPC3 isoforms, TRPC1 and TRPC6, but showed significantly decreased TRPC4 expression. TRPC4 anchors to the dystrophin-associated protein complex and is necessary to maintain the normal regulation of extracellular Ca^{2+}-entry in skeletal muscle (Sabourin *et al*., 2009). Possibly the decreased TRPC4 expression in myoblast state is one of auxiliary factors inducing high Ca^{2+} content in the SR of MDG/TRPC3 KD myoblasts. However the molecular mechanism how TRPC4 is correlated to TRPC3 and contributes to inducing high SR Ca^{2+} content is not clear yet. Another extracellular Ca^{2+}-entry channel, Orai1 was also down-regulated in MDG/TRPC3 KD myoblasts. Orai1 negatively regulates TRPC3 function by physical interactions (Liao *et al*., 2007). It is possible that TRPC3 knock-down in MDG/TRPC3 KD myoblasts could induce down-regulation of its counterpart protein, Orai1.

Taken together, we suggest that TRPC3 (possibly Ca^{2+}-entry via TRPC3) plays an important role in the maintenance of skeletal muscle myoblasts and myotubes. Further study on a detailed functional correlation among TRPC3, DHPR, MG29, TRPC4, and Orai1 in conjunction with intracellular Ca^{2+} homeostasis will improve our understanding how these proteins contribute to physiological and patho-physiological processes of skeletal muscle.

Methods

Materials

Fetal bovine serum, F-10 nutrient mixture, L-glutamine, penicillin/streptomycin, low- and high-glucose Dulbecco's Modified Eagle's Medium, and basic fibroblast growth factor were obtained from Invitrogen. Anti-TRPC1, TRPC3, TRPC4, and TRPC6 antibodies were obtained from Alomone Laboratories. Anti-STIM1, anti-Orai1, anti-p53, and anti-caspase-3 antibodies were obtained from Cell Signaling. Anti-desmin antibody was obtained from DakoCytomation. Cy-3-conjugated anti-mouse IgG antibody and normal goat serum (NGS) were obtained from Jackson ImmunoResearch. Anti-MG29 antibody was obtained from Santa Cruz Biotechnology. Matrigel was obtained from BD Biosciences. Cyclopiazonic acid (CPA), caffeine, KCl, horse serum, and collagen were obtained from Sigma-Aldrich. Ethyl-1-(4-(2,3,3-trichloroacrylamide)phenyl)-5-(trifluoromethyl)-1H-pyrazole-4-carboxylate (Pyr3) was obtained from Tocris.

Cell cultures

Primary wild-type or $\alpha 1_S$DHPR-null muscular dysgenic (MDG) myoblasts were derived from wild-type or MDG mouse skeletal muscle, respectively, as previously described (Flucher *et al*., 1993; Felder *et al*., 2002). Primary wild-type, MDG, or MDG/TRPC3 KD myoblasts, or HEK293 cells were cultured as previously described (Lee *et al*., 2004, 2006a, 2006c; Woo *et al*., 2010). All surgical interventions and pre- and post-surgical animal care were provided in accordance with the Laboratory Animals Welfare Act, the Guide for the Care and Use of Laboratory Animals, and the Guidelines and Policies for Rodent Survival Surgery provided by the Institutional Animal Care and Use Committee of the College of Medicine, The Catholic University of Korea.

Clonal selection of MDG/TRPC3 KD myoblast line

To derive the MDG/TRPC3 KD myoblast line, we knocked down the mRNA of TRPC3 in MDG myoblasts using retrovirus-delivered small interference RNAs (Lee *et al*., 2006a). First, two different sequences were selected using a program from Dharmacon siDESIGN center (Dharmacon, Thermo Fisher Scientific) based on the cDNA sequence of TRPC3 (GenBank accession number NM_019510). BLAST searches confirmed that the selected oligonucleotide sequences did not possess homology to any other genes. Each of two 19-nucleotide sequences (Figure 1A, Sequences I and II) was inserted into a retroviral vector (pSIREN-RetroQ, Clontech Laboratories, Inc.) using the 5'-BamH I and 3'-EcoR I sites. Retroviral particles were packaged by transfecting each short hairpin RNA-expressing vector into HEK293-based packaging cells with FuGENE transfection reagent (Roche), and the harvested supernatant was filtered with 0.2 μm non-pyrogenic disc filters (Pall Corporation). Filter-through containing the retroviral particles (MDG/TRPC3 KD retroviruses I or II) was stored at -70°C before use. MDG myoblasts were infected with both MDG/TRPC3 KD retroviruses I and II and polybrene (8 μg/ml) for 3 h. Successfully infected myoblasts were clonally selected using puromycin (0.3 μg/ml) on 3 successive days after the infection. Each selected clone was subjected to proliferation or differentiation into myotubes described in Cell Cultures. Wild-type myoblasts infected with the empty retroviruses were used as negative controls in subsequent experiments (data not shown).

Evaluation of TRPC3 mRNA level in MDG/TRPC3 KD myoblasts by real-time PCR

Total cellular RNA of wild-type myoblasts or ten selected

TRPC3 knock-down and DHPR-null myoblast clones was extracted from 5×10^5 cells, digested with RNase-free DNase I, and reverse-transcribed into cDNAs using a Sensiscript RT kit and random primers according to the manufacturer's protocol (Invitrogen). TRPC3 mRNA levels were analyzed using real-time PCR with the reverse-transcribed cDNAs. mRNA levels of glyceraldehyde-3-phosphate dehydrogenase (GAPDH) were used as positive controls. Real-time PCR was carried out in optical 96-well plates using the SYBR green master mix. The primers were as follows: TRPC3, 5'-GCCAAGCGACGGAGGAATTA-3' (forward primer) and 5'-CAGCACACTGGGGTTCAGTT-3' (reverse primer); GAPDH, 5'-TTGTCAAGCTCATTTCCTGGTATG-3' (forward primer) and 5'-GCCATGTAGGCCATGAGGTC-3' (reverse primer). Transcription of each gene was assayed in triplicate in a total volume of 20 μl containing 1× SYBR green reagent, 10 nM of each gene-specific primer pair, and 50 ng of cDNAs. The thermal profile for amplification was as follows: 50°C for 2 min, 95°C for 10 min, and 40 cycles of 95°C for 30 s, 60°C for 30 s, and 72°C for 30 s. Amplification and detection were performed using a Prism 7900 HT sequence detection system (Applied Biosystems).

Single myoblast Ca^{2+} imaging experiments and preparation of cell images

Ca^{2+} transients, the SR Ca^{2+} contents, and resting cytosolic Ca^{2+} levels were measured in wild-type, MDG, or MDG/TRPC3 KD myoblasts loaded with 5 μM fura-2-AM (Molecular Probes, Invitrogen) in an imaging buffer (125 mM NaCl, 5 mM KCl, 2 mM KH_2PO_4, 2 mM $CaCl_2$, 25 mM HEPES, 6 mM glucose, 1.2 mM $MgSO_4$, and 0.05% BSA (fraction V) at pH 7.4.) at 37°C for 45 min as previously described (Lee *et al*., 2004, 2006c). Fura-2 in the myotubes was excited at 340 nm and 380 nm, and fluorescence emission was measured at 510 nm using High-Speed InCyt Im2 image acquisition system and analysis software (v5.29; Intracellular Imaging, Inc). Intracellular Ca^{2+} concentrations were calculated as described by Grynkiewicz *et al*. (using 225 nM as the Ca^{2+}-fura-2 dissociation constant) (1985). CPA was dissolved in Me_2SO ($< 0.05\%$) and manually applied to myoblast. Me_2SO (0.05%) alone had no effect on Ca^{2+} transients. For Pyr3 treatment, Pyr3 dissolved in Me_2SO ($< 0.05\%$) was incubated with MDG myoblasts in the imaging buffer for 45 min before Ca^{2+} imaging. To analyze the Ca^{2+} transients obtained from the Ca^{2+} imaging experiments, peak area was considered. To examine morphological changes, images of wild-type and MDG/TRPC3 KD myoblasts on 10-cm dishes coated with collagen or images of myoblasts/myotubes during differentiation on optic 96-well plates coated with Matrigel were captured using an inverted microscope (IX71, Olympus).

Immunohistochemistry

Wild-type or MDG/TRPC3 KD myoblasts were fixed in cold methanol (-20°C) for 15 min and permeabilized with 0.05% Tween 20 in phosphate-buffered saline (PBS) for 1 min. After blocking myoblasts with 2% NGS in PBS, myoblasts were incubated with anti-desmin antibody (1:100) for 3 h at 25°C, washed with 2% NGS in PBS for 10 min, incubated with Cy-3-conjugated anti-mouse IgG antibody (1:5000) for 45 min at 25°C, and visualized with a fluorescence inverted microscope (IX71, Olympus, 550 nm excitation and 570 nm emission).

Preparation of myoblast lysate and immunoblot assay

Myoblasts grown on 10-cm culture dishes were solubilized by addition of 300 μl lysis buffer (1% Triton X-100, 10 mM Tris-HCl (pH 7.4), 1 mM Na_3VO_4, 10% glycerol, 150 mM NaCl, 5 mM EDTA, and protease inhibitors (1 μM pepstatin, 1 μM leupeptin, 1 mM phenylmethylsulfonyl fluoride, 20 mg/ml aprotinin, and 1 μM trypsin inhibitor)) per a 10-cm culture dish, followed by incubation overnight at 4°C with gentle mixing (Lee *et al*., 2006a; Woo *et al*., 2008). The final protein concentration of the solubilized lysate was determined by the Bradford method by using bovine serum albumin as the standard. The solubilized lysate (30 μg total proteins) was boiled in sodium dodecyl sulfate (SDS) sample buffer followed by 10% or 12% polyacrylamide gel electrophoresis (PAGE) for immunoblot assay with anti-TRPC1 (1:800), anti-TRPC3 (1:800), anti-TRPC4 (1:800), anti-TRPC6 (1:800), anti-STIM1 (1:1000), anti-Orai1 (1:1000), anti-p53 (1:1000), anti-caspase-3 (1:1000), or anti-MG29 antibody (1:2000).

Myoblast count and BrdU-incorporation assay

The number of wild-type or MDG/TRPC3 KD myoblasts per unit area was counted under the microscope. MDG/TRPC3 KD myoblasts containing multi-nuclei were counted as single cells. BrdU-incorporation assay was performed with wild-type or MDG/TRPC3 KD myoblasts grown on Matrigel-coated 96-well plates using a BrdU immunohistochemistry kit according to the manufacturer's protocol (Chemicon International, Inc.). Briefly, myoblasts were incubated with BrdU (10 μM) for 4 h. Myoblasts incorporating BrdU were visualized by immunohistochemistry with biotinylated anti-BrdU antibody (1:200 dilution in 0.1% BSA in PBS), streptavidin-HRP conjugate secondary antibody (1:500), and diaminobenzidine. The number of BrdU-stained cells as a percentage of total cells was determined.

DNA fragmentation assay

DNA fragmentations in myoblasts and myotubes were assayed by an apoptotic DNA ladder detection kit according to the manufacturer's protocol (Millipore). Approximately 5×10^5 cells were subjected to the genomic DNA isolation and the isolated genomic DNAs were loaded on an ethidium bromide-treated 1.5% agarose gel.

Statistical analysis

Results are presented as means ± SE with the number of experiments indicated in the figure legends. Significant differences were analyzed using paired *t*-tests (GraphPad InStat, v2.04). Differences were considered to be signi-

ficant at $P < 0.05$. Graphs were prepared using Origin v7.

Supplemental data

Supplemental Data include three figures and can be found with this article online at http://e-emm.or.kr/article/article_files/SP-42-9-3.pdf.

Acknowledgements

This work was supported by the Korea Research Foundation Grant funded by the Korean Government (MOEHRD) (KRF-2008-331-E00011), and by a grant of the Korea Healthcare-Technology R&D Project, Ministry of Health & Welfare, Republic of Korea (A090047). We wish to acknowledge the help of Dr. Paul D. Allen (Department of Anesthesiology, Perioperative and Pain Medicine, Brigham and Women's Hospital, Harvard Medical School, Boston, MA) for supplying MDG myoblasts and editorial assistance.

References

Abramowitz J, Birnbaumer L. Physiology and pathophysiology of canonical transient receptor potential channels. FASEB J 2009;23:297-328

Alberts B. Molecular Biology of the Cell, 2008, Garland Science, New York, USA

Benchimol S. p53-dependent pathways of apoptosis. Cell Death Differ 2001;8:1049-51

Brotto MA, Nagaraj RY, Brotto LS, Takeshima H, Ma JJ, Nosek TM. Defective maintenance of intracellular Ca^{2+} homeostasis is linked to increased muscle fatigability in the MG29 null mice. Cell Res 2004;14:373-8

Felder E, Protasi F, Hirsch R, Franzini-Armstrong C, Allen PD. Morphology and molecular composition of sarcoplasmic reticulum surface junctions in the absence of DHPR and RyR in mouse skeletal muscle. Biophys J 2002;82:3144-9

Fernando P, Kelly JF, Balazsi K, Slack RS, Megeney LA. Caspase 3 activity is required for skeletal muscle differentiation. Proc Natl Acad Sci USA 2002;99:11025-30

Flucher BE, Andrews SB, Fleischer S, Marks AR, Caswell A, Powell JA. Triad formation: organization and function of the sarcoplasmic reticulum calcium release channel and triadin in normal and dysgenic muscle in vitro. J Cell Biol 1993;123:1161-74

Freichel M, Vennekens R, Olausson J, Stolz S, Philipp SE, Weissgerber P, Flockerzi V. Functional role of TRPC proteins in native systems: implications from knockout and knock-down studies. J Physiol 2005;567:59-66

Grynkiewicz G, Poenie M, Tsien RY. A new generation of Ca^{2+} indicators with greatly improved fluorescence properties. J Biol Chem 1985;260:3440-50

Hartmann J, Dragicevic E, Adelsberger H, Henning HA, Sumser M, Abramowitz J, Blum R, Dietrich A, Freichel M, Flockerzi V, Birnbaumer L, Konnerth A. TRPC3 channels are required for synaptic transmission and motor coordination. Neuron 2008;59:392-8

Hofmann T, Obukhov AG, Schaefer M, Harteneck C, Gudermann T, Schultz G. Direct activation of human TRPC6 and TRPC3 channels by diacylglycerol. Nature 1999;397:259-63

Jia Y, Zhou J, Tai Y, Wang Y. TRPC channels promote cerebellar granule neuron survival. Nat Neurosci 2007;10:559-67

Kiselyov K, Patterson RL. The integrative function of TRPC channels. Front Biosci 2009;14:45-58

Kiyonaka S, Kato K, Nishida M, Mio K, Numaga T, Sawaguchi Y, Yoshida T, Wakamori M, Mori E, Numata T, Ishii M, Takemoto H, Ojida A, Watanabe K, Uemura A, Kurose H, Morii T, Kobayashi T, Sato Y, Sato C, Hamachi I, Mori Y. Selective and direct inhibition of TRPC3 channels underlies biological activities of a pyrazole compound. Proc Natl Acad Sci USA 2009;106:5400-5

Klaus MM, Scordilis SP, Rapalus JM, Briggs RT, Powell JA. Evidence for dysfunction in the regulation of cytosolic Ca2+ in excitation-contraction uncoupled dysgenic muscle. Dev Biol 1983;99:152-65

Lee EH, Lopez JR, Li J, Protasi F, Pessah IN, Kim DH, Allen PD. Conformational coupling of DHPR and RyR1 in skeletal myotubes is influenced by long-range allosterism: evidence for a negative regulatory module. Am J Physiol Cell Physiol 2004;286:C179-89

Lee EH, Cherednichenko G, Pessah IN, Allen PD. Functional coupling between TRPC3 and RyR1 regulates the expressions of key triadic proteins. J Biol Chem 2006a;281:10042-8

Lee EH, Kim DH, Allen PD. Interplay between intra- and extracellular calcium ions. Mol Cells 2006b;21:315-29

Lee EH, Song DW, Lee JM, Meissner G, Allen PD, Kim DH. Occurrence of atypical Ca2+ transients in triadin-binding deficient-RYR1 mutants. Biochem Biophys Res Commun 2006c;351:909-14

Lee EH, Allen PD. Homo-dimerization of RyR1 C-terminus via charged residues in random coils or in an alpha-helix. Exp Mol Med 2007;39:594-602

Li HS, Xu XZ, Montell C. Activation of a TRPC3-dependent cation current through the neurotrophin BDNF. Neuron 1999;24:261-73

Li Y, Jia YC, Cui K, Li N, Zheng ZY, Wang YZ, Yuan XB. Essential role of TRPC channels in the guidance of nerve growth cones by brain-derived neurotrophic factor. Nature 2005;434:894-8

Liao Y, Erxleben C, Yildirim E, Abramowitz J, Armstrong DL, Birnbaumer L. Orai proteins interact with TRPC channels and confer responsiveness to store depletion. Proc Natl Acad Sci USA 2007;104:4682-7

Lof C, Blom T, Tornquist K. Overexpression of TRPC3 reduces the content of intracellular calcium stores in HEK-293 cells. J Cell Physiol 2008;216:245-52

Lyfenko AD, Dirksen RT. Differential dependence of

store-operated and excitation-coupled Ca^{2+} entry in skeletal muscle on STIM1 and Orai1. J Physiol 2008;586:4815-24

McKay RR, Szymeczek-Seay CL, Lievremont JP, Bird GS, Zitt C, Jungling E, Luckhoff A, Putney JW Jr. Cloning and expression of the human transient receptor potential 4 (TRP4) gene: localization and functional expression of human TRP4 and TRP3. Biochem J 2000;351 Pt 3:735-46

Millay DP, Goonasekera SA, Sargent MA, Maillet M, Aronow BJ, Molkentin JD. Calcium influx is sufficient to induce muscular dystrophy through a TRPC-dependent mechanism. Proc Natl Acad Sci USA 2009;106:19023-8

Nakai J, Dirksen RT, Nguyen HT, Pessah IN, Beam KG, Allen PD. Enhanced dihydropyridine receptor channel activity in the presence of ryanodine receptor. Nature 1996;380:72-5

Nilius B, Owsianik G, Voets T. Transient receptor potential channels meet phosphoinositides. EMBO J 2008;27: 2809-16

Nishida M, Sugimoto K, Hara Y, Mori E, Morii T, Kurosaki T, Mori Y. Amplification of receptor signalling by Ca^{2+} entry-mediated translocation and activation of PLCgamma2 in B lymphocytes. EMBO J 2003;22:4677-88

Paulin D, Li Z. Desmin: a major intermediate filament protein essential for the structural integrity and function of muscle. Exp Cell Res 2004;301:1-7

Pedersen SF, Owsianik G, Nilius B. TRP channels: an overview. Cell Calcium 2005;38:233-52

Philipp S, Strauss B, Hirnet D, Wissenbach U, Mery L, Flockerzi V, Hoth M. TRPC3 mediates T-cell receptor-dependent calcium entry in human T-lymphocytes. J Biol Chem 2003;278:26629-38

Pigozzi D, Ducret T, Tajeddine N, Gala JL, Tombal B, Gailly P. Calcium store contents control the expression of TRPC1, TRPC3 and TRPV6 proteins in LNCaP prostate cancer cell line. Cell Calcium 2006;39:401-15

Preston SF, Sha'afi RI, Berlin RD. Regulation of Ca^{2+} influx during mitosis: Ca^{2+} influx and depletion of intracellular Ca^{2+} stores are coupled in interphase but not mitosis. Cell Regul 1991;2:915-25

Ramsey IS, Delling M, Clapham DE. An introduction to TRP channels. Annu Rev Physiol 2006;68:619-47

Reading SA, Earley S, Waldron BJ, Welsh DG, Brayden JE. TRPC3 mediates pyrimidine receptor-induced depolarization of cerebral arteries. Am J Physiol Heart Circ Physiol 2005;288:H2055-61

Sabourin J, Lamiche C, Vandebrouck A, Magaud C, Rivet J, Cognard C, Bourmeyster N, Constantin B. Regulation of TRPC1 and TRPC4 cation channels requires an alpha1-syntrophin-dependent complex in skeletal mouse myotubes. J Biol Chem 2009;284:36248-61

Sampieri A, Diaz-Munoz M, Antaramian A, Vaca L. The foot structure from the type 1 ryanodine receptor is required for functional coupling to store-operated channels. J Biol Chem 2005;280:24804-15

Sandow A. Excitation-contraction coupling in skeletal muscle. Pharmacol Rev 1965;17:265-320

Santillan G, Baldi C, Katz S, Vazquez G, Boland R. Evidence that TRPC3 is a molecular component of the 1alpha,25(OH)2D3-activated capacitative calcium entry (CCE) in muscle and osteoblast cells. J Steroid Biochem Mol Biol 2004;89-90:291-5

Siu PM, Alway SE. Mitochondria-associated apoptotic signalling in denervated rat skeletal muscle. J Physiol 2005; 565:309-23

Soddu S, Blandino G, Scardigli R, Coen S, Marchetti A, Rizzo MG, Bossi G, Cimino L, Crescenzi M, Sacchi A. Interference with p53 protein inhibits hematopoietic and muscle differentiation. J Cell Biol 1996;134:193-204

Stiber J, Hawkins A, Zhang ZS, Wang S, Burch J, Graham V, Ward CC, Seth M, Finch E, Malouf N, Williams RS, Eu JP, Rosenberg P. STIM1 signalling controls store-operated calcium entry required for development and contractile function in skeletal muscle. Nat Cell Biol 2008;10:688-97

Tanaka H, Furuya T, Kameda N, Kobayashi T, Mizusawa H. Triad proteins and intracellular Ca^{2+} transients during development of human skeletal muscle cells in aneural and innervated cultures. J Muscle Res Cell Motil 2000;21:507-26

Tassin AM, Pincon-Raymond M, Paulin D, Rieger F. Unusual organization of desmin intermediate filaments in muscular dysgenesis and TTX-treated myotubes. Dev Biol 1988;129: 37-47

Van Assche T, Fransen P, Guns PJ, Herman AG, Bult H. Altered Ca^{2+} handling of smooth muscle cells in aorta of apolipoprotein E-deficient mice before development of atherosclerotic lesions. Cell Calcium 2007;41:295-302

Vandebrouck C, Martin D, Colson-Van Schoor M, Debaix H, Gailly P. Involvement of TRPC in the abnormal calcium influx observed in dystrophic (mdx) mouse skeletal muscle fibers. J Cell Biol 2002;158:1089-96

Vazquez G, Lievremont JP, St JBG, Putney JW Jr. Human Trp3 forms both inositol trisphosphate receptor-dependent and receptor-independent store-operated cation channels in DT40 avian B lymphocytes. Proc Natl Acad Sci USA 2001; 98:11777-82

Vazquez G, Wedel BJ, Trebak M, St John Bird G, Putney JW, Jr. Expression level of the canonical transient receptor potential 3 (TRPC3) channel determines its mechanism of activation. J Biol Chem 2003;278:21649-54

Vig M, DeHaven WI, Bird GS, Billingsley JM, Wang H, Rao PE, Hutchings AB, Jouvin MH, Putney JW, Kinet JP. Defective mast cell effector functions in mice lacking the CRACM1 pore subunit of store-operated calcium release-activated calcium channels. Nat Immunol 2008;9: 89-96

Weisleder N, Brotto M, Komazaki S, Pan Z, Zhao X, Nosek T, Parness J, Takeshima H, Ma J. Muscle aging is associated with compromised Ca^{2+} spark signaling and segregated intracellular Ca^{2+} release. J Cell Biol 2006;174:639-45

Woo JS, Kim DH, Allen PD, Lee EH. TRPC3-interacting triadic proteins in skeletal muscle. Biochem J 2008;411: 399-405

Woo JS, Hwang JH, Ko JK, Weisleder N, Kim DH, Ma J, Lee

EH. S165F mutation of junctophilin 2 affects Ca^{2+} signalling in skeletal muscle. Biochem J 2010;427:125-34

Wu X, Eder P, Chang B, Molkentin JD. TRPC channels are necessary mediators of pathologic cardiac hypertrophy. Proc Natl Acad Sci USA 2010;107:7000-5

Yildirim E, Kawasaki BT, Birnbaumer L. Molecular cloning of TRPC3a, an N-terminally extended, store-operated variant of the human C3 transient receptor potential channel. Proc Natl Acad Sci USA 2005;102:3307-11

Zanou N, Shapovalov G, Louis M, Tajeddine N, Gallo C, Van Schoor M, Anguish I, Cao ML, Schakman O, Dietrich A, Lebacq J, Ruegg U, Roulet E, Birnbaumer L, Gailly P. Role of TRPC1 channel in skeletal muscle function. Am J Physiol Cell Physiol 2010;298:C149-62

Zhao X, Weisleder N, Thornton A, Oppong Y, Campbell R, Ma J, Brotto M. Compromised store-operated Ca^{2+} entry in aged skeletal muscle. Aging Cell 2008;7:561-8

Zhu X, Jiang M, Birnbaumer L. Receptor-activated Ca^{2+} influx via human Trp3 stably expressed in human embryonic kidney (HEK)293 cells. Evidence for a non-capacitative Ca^{2+} entry. J Biol Chem 1998;273:133-42